Ductile Fracture Behaviour under Mode I Loading Using Rousellier Ductile Damage Theory

Dong-Joon Oh*
Korea Atomic Energy Research Institute, Korea
I. C. Howard, J. R. Yates
The university of Sheffield, UK

The aim of this study is to investigate the ductile fracture behaviour under Mode I loading using SA533B pressure vessel steel. Experiments consist of the Round Notch Bar Test (RNB), Single Edge Crack Bending Test (SECB), and V-Notch Bar Test (VNB). Results from the RNB test were used to tune the damage modelling constant. The other tests were performed to acquire the J-resistance curves and to confirm the damage constants. Microstructural observation includes the measurement of crack profile to obtain the roughness parameter. Finally, simulation using Rousellier Ductile Damage Theory (RDDT) was carried out with 4-node quadrilateral element (L_c=0.25 mm). For the crack advance, the failed element removal technique was adopted with a β criterion. In conclusion, the predicted simulation using RDDT showed a good agreement with the experimental results. A trial using a roughness parameter was made for a new evaluation of J-resistance curve, which is more conservative than the conventional one.

Key Words : RDDT(Rousellier Ductile Damage Theory), Ductile Fracture, J-Resistance, Roughness Parameter, SA533B Pressure Vessel Steel

1. Introduction

Ductile fracture behaviour of pressure vessel steel, that is most popular in power plant (Han -Ki Yoon et al., 1999), is closely related to the growth of micro-voids. As the micro-voids are nucleated and coalescenced, materials can not endure the designed strength. After this material becomes degraded, it will finally be failed. Generally, the degression of material results from the relationship between the mechanism of micro-void growth and the secondary particles.

Even though damage mechanics (DM) does not use the fracture toughness parameter such as K or J, DM makes it possible to express the damage and failure of material using continuum mechanics. It is another expression of material strength related to the micro-void growth around the secondary particles which are the major defect in ductile fracture.

Damage mechanics explains the micro-void mechanism as the expression of 'Cell'. As the cells are degraded and failed, they are characterized using the constitutive equation in continuum mechanics. While a crack tip is represented as the array of cells, they are deformed by obeying of plastic theory. If the first cell is applied by the maximum load, the micro-voids are nucleated in the cell and begin to degrade. After this cell is damaged and failed, the spared load of the second cell in front of the crack tip causes the micro-void growth. This process takes place in the next cells repeatedly. Rousellier Ductile Damage Theory (RDDT) used for this study, is introduced briefly in the next section.

* Corresponding Author,
E-mail : ex-djoh@nanum.kaeri.re.kr
TEL : +82-42-868-8006 ; **FAX** : +82-42-868-8346
Korea Atomic Energy REsearch Institute, P. O. Box 105, Yusong, Taejon 305-600, Korea.(Manuscript **Received** March 11, 2000 ; **Revised** June 5, 2000)

2. Rousellier Ductile Damage Theory (RDDT)

The details of RDDT are explained in references (Rousellier, 1987 ; Bilby et al., 1987). The plastic potential, F, can be expressed as

$$F=F_h+F_s=\frac{\sigma}{\rho}+\sqrt{3}B(\beta)De^{\frac{C\sigma_m}{\rho\sigma_Y}} \quad (1)$$

The damage function $B(\beta)$ can be determined from Eq. (2)

$$B(\beta)=\sigma_Y f_0\frac{e^{\beta}}{C(1-f_0+e^{\beta})} \quad (2)$$

$$\beta=ln\{f(1-f_0)/f_0(1-f)\}$$

F: plastic potential

σ_{eq}: the equivalent stress

ρ: the density

σ_m: the mean stress

σ_Y: the yield stress

β, C, D: the damage parameters

f, f_0: the current and initial values of void volume fraction.

3. Experimental Methods

3.1 Material

The material tested in this study was obtained from an SA533B, Type B, Class 1 forged plate which had the dimension of 70(t) 2500(w) 2500 (l) mm. The heat treatments and the chemical composition of SA533B/C1 are given in Table 1 and Table 2 respectively.

Table 1 Heat treatment of A533B / C1

Heat Treatment	Temperature(℃)	Period	Cooling
Austenise	870-908	4hr. 17min	Water Quenohed
Temper	650-660	6hr. 40min	Air Cooled

Table 2 Chemical comnposition($wt.\%$) ofA533B/C1

C	Si	Mn	S	P	Cr	Mo	Ni	V	Cu
0.21	0.26	1.4	0.018	0.006	0.10	0.50	0.66	0.003	0.04

Three tensile specimen were used to determine the load versus displacement curve to obtain values of 0.2% yield strength (533.8 MPa) and the ultimate tensile strength (660.1 MPa). The geometry of the tensile specimen is the same as the round notch bar (RNB) specimen except the round notch. The elongation (18.3%). the Young's modulus (213.8 GPa) and the Poisson's ratio (0.281) were also obtained using the Shenck Machine (PM 250KN). The true stress versus true strain curve is shown in Fig. 1 and it was also used in the simulation of RDDT.

3.2 RNB test

Figure 2 shows the geometry of round notch (10 mm) bar specimen tested. For this study, each five RNB specimens were tested for 10 mm and 4 mm round notch. The radial and axial extensions were recorded using the radial and axial extensometers (Fig. 3).

3.3 Mode I test

3.3.1 VNB test

The main objective of this test is the validation of the damage theory that has been chosen as the

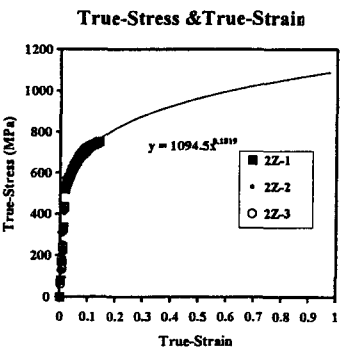

Fig. 1 True stress vs. true strain

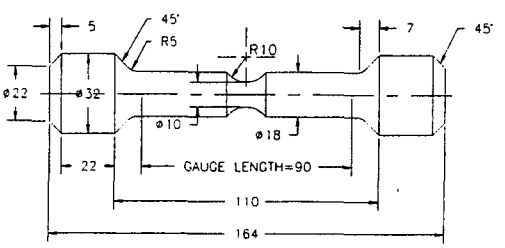

Fig. 2 RNB with a 10mm round notch

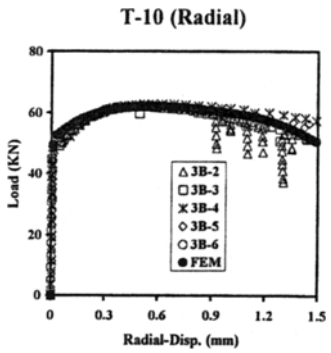

Fig. 3 Load (KN) vs. radial disp. (mm) of RNB-10

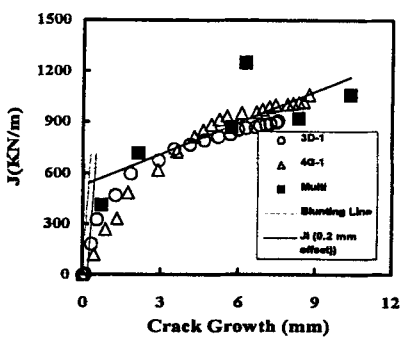

Fig. 4 J-resistance curves under mode I loading

basis for numerical analysis to be performed in this study later. For this purpose a tensile bar fracture toughness test was carried out using axisymmetric V-notch tensile bar specimens. Fatigue pre-cracking was carried out by the Suresh's cyclic compression method (Suresh et al., 1987) and the crack measurement was made by the Hay's DCPD method (Hay etal., 1981). J values were calculated by the Devaux (1985) Eq. (3).

$$J=K^2(1-\nu^2)/E+P\delta_p/2\pi R_0^2 \qquad (3)$$
$$\delta_p=\delta-CP$$

P : the applied load
δ_p : the plastic displacement
δ : the total displacement
R_0: the initial radius of the uncracked ligament
C : the compliance

The VNB test results were marked by some parts of the multiple specimen method results as (■) symbol in Fig. 4.

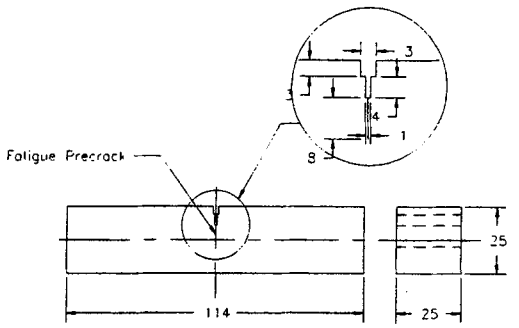

Fig. 5 SECB specimen (W=25 mm)

3.3.2 SECB Test

Figure 5 shows the SECB specimen with a square cross-section. Its span to width ratio (S/W) is 4 and the original crack size is equal to 0.6W. Two width of 25 mm and 50 mm were used. In the former case, the five specimens were tested by single and multiple specimen method, but for the latter case, one specimen was tested as specified by the single specimen method. This test was conducted in displacement control mode using the electrically-driven Mayes machine (SM 100). The SECB tests were carried out in accordance with BS 7448 and EGF P-90. The crack growth was monitored by the DCPD method and the physical crack length after fracture, was measured and compared. J values were calculated using the Eq. (4).

$$J_0=\eta U/B_n(W-a_0),$$
$$J=J_0\{1-(0.75\eta-1)\Delta a/(W-a_0)\} \qquad (4)$$

$\eta=2$ for SECB specimen
B_n: the net thickness of the specimen
W: the specimen width
a_0: the initial crack length
U: the area under the load vs. load disp
Δa: the increment of crack growth

The J-R curves of SECB are shown in Fig. 4. (○) symbol represents the results of SECB-25 and (△) symbol means the results of SECB -50.

4. Microstructural Observation

4.1 Examination of MnS

To define the cell size of the RDDT simulation, the length and distance of metallic inclusions

Fig. 6 Crack Profile Showing Micro-void Nucleation and Coalescence

were examined. MnS(Manganese Sulphide) inclusions were mainly observed and confirmed by the X-ray analysis using EDS (Electron dispersive spectroscopy). The volume fraction of MnS on the L-Face was measured using Image Analyser. This value (f_v=0.102 %) is very similar to that (f_v=0.0933 %) of Franklin's equation (Franklin, 1969). Since the average spacing is about 0.26 mm, the cell size is defined as 0.25 mm.

4.2 Linear roughness parameter: R_L

The stress concentration of inclusion such as MnS under Mode I loading results in the nucleation and coalescence of micro-voids. The path of crack propagation is not straight but irregular in Fig. 6. Because the crack propagates along the weakest sites where the micro-voids nucleate and coalescence. Therefore, the true crack length (a_t) is longer than the measured crack length (projected crack length: a_p). A Linear roughness parameter, RL, is defined as(Underwood et al., 1985)

$$R_L = a_t / a_p. \tag{5}$$

It was known that R_Ls were material constant if the state of stress distribution and geometry were equal. R_Ls of VNB and SECB (25,50 mm) are 1.092, 1.483, and 1.447, respectively. Even though the VNB and SECB specimen were subjected to the same mode I loading, each R_L was different because the geometry was not equal and the plain strain state of SECB is different from the axisymmetric stress state of VNB. However, the roughnesses of two SECB specimens with different thickness did not show a distinct difference due to the similarity of stress state and geometry.

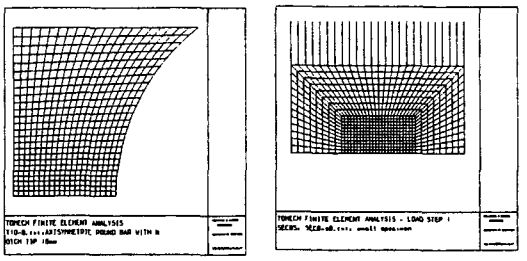

Fig. 7 The mesh of RNB-10 and SECB-25

5. Simulations Using RDDT

TOMECH has been developed within the department of Mechanical Engineering at the University of Sheffield to simulate the elastic-plastic finite element analyses using RDDT. For these analyses, some necessary parameters such as mesh type and size, mechanical properties, inclusion volume fraction, the constants of RDDT, and the β constant for the criteria of damage, were determined. The adopted mesh is the 4-node quadrilaterl element (0.25 mm). Figure 7 shows the crack tip mesh of RNB-10 and SECB-25 specimen.

Since MnS volume fraction from the metallographic observation, is very similar to that of Franklin's experimental equation, 0.102% was adopted for this simulation. The true stress versus true strain relationship used in the elastic-plastic analyses was determined experimentally and input to the code as 24 pairs of data points from the experimental curve.

The parameters C and D are initially tuned by simulating the load versus notch root diametrical contraction curves of RNB specimens. These values of C(1.6) and D(2.0) are confirmed by obtaining the J-R curves of the VNB and SECB tests. (●) symbol in Fig. 3 denotes the FEM results using RDDT and is compared with the test results.

The β criterion was used for crack advance. β_{crit} value (5.5) was tuned and confirmed using the J-R curves or the load versus load displacement relation from VNB and SECB tests. If value of the finite elements is over β_{crit}, these finite elements are considered as the damaged elements and removed from calculation. This crack

advance method is called the failed element removal technique.

Figwes 8 and 9 demonstrate the comparison of load versus load displacement curves and J-R curves between the test data and FEM prediction, respectively.

The FEM prediction for SECB-25 in Fig. 8 shows a very good agreement with the test data. While the points in Fig. 9 denote the test data, the lines mean the FEM prediction. After the cracks initiate, the test data located between the predicted FEM Lines. As the load was increased, the β values of the first six elements in front of the crack tip were changed in Fig. 10. After the β value of the first element was over β_{crit} and the load was increased, the remaining elements approached to β_{crit} in turn.

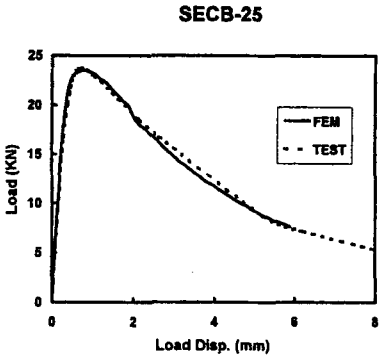

Fig. 8 The Comparison of Load vs. Load Displacement Curve between SECB-25 Test Result and FEM Prediction

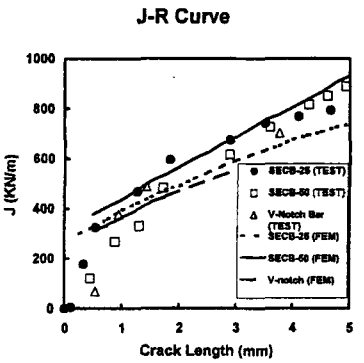

Fig. 9 The Comparison of J-resistance Curves between SECB-25, 50 and VNB Test Data and FEM Prediction

6. Discussion

6.1 J-R curves using the true crack length obtained from R_L

If the characteristics of fracture surface is well-known, many unsolved problem in fracture mechanics will be sorted out. It is clear that the true crack length is longer than the conventional crack length (that is called the projected crack length). The true crack length was able to be calculated using the linear roughness parameter obtained from the crack profile (refer to Eq. 4).

A new attempt to analyse the fracture toughness of ductile materials is to use the true crack length (a_t) instead of the conventional crack length (the projected crack length: a_p).

Figure 11 shows the J resistance curves using the true crack length, a_t. This figure shows that

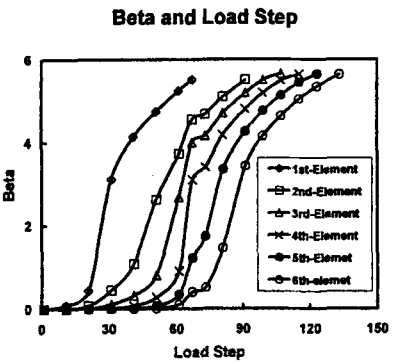

Fig. 10 β value vs. load step at the first six elements of crack tip front ($\beta_{crit}=5.5$)

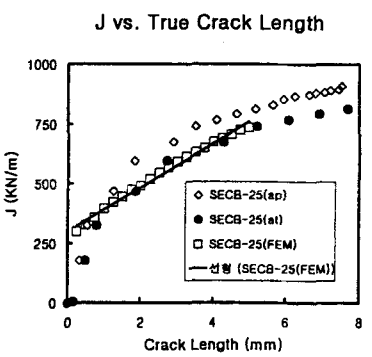

Fig. 11 Comparison of the predicted and measured J-R curves obtained from using true and projected crack length for SECB-25

the fracture toughness is decreased when using the true crack length instead of using of the projected crack length, a_p. It is interesting to note that the predicted J resistance curve (Line: —) for Mode I loading using Rousellier damage theory, is in better agreement with that (●) of the true crack length rather than the projected crack length (◇). It suggests that in order to avoid the overestimation of conventional J resistance curves of the projected crack length, J resistance curve of the true crack length is more practical and conservative than the conventional one.

6.2 Damage Parameter, β

With the usual hypothesis of constant volume plastic deformation, it is possible to ignore the variation of density, but if the ductile damage theory is adopted the variation of density should be considered. If there is no damage, density (ρ) will be constant and the only changes of density are the small ones due to the elastic deformation. If ρ is variable, the variation of β depends on the density. It was shown that the expression for β is very similar to the void growth ratio β and they expected the prediction using and void growth ratio as criteria for crack advance to be similar (Li et al., 1994). A physical connection between β and void growth was indicated by the theory and they also claimed that a criterion for crack advance controlled by the attainment of a specific value of β is connected with the growth of voids to a specific size.

β_{crit} under Mode I loading is 5, 5 and is not relevant to the specimen geometry. It is also implied that β value just depends on the loading condition.

7. Conclusions

The ductile fracture behaviour under Mode I loading using SA533B pressure vessel steel was investigated. Experiments of RNB, VNB and SECB, metallographic examination and the prediction of RDDT were performed. By the comparison between the test data and the predicted results, the following conclusions were obtained.

(1) When using RDDT, β_{crit} is 5.5 under Mode I loading and does not depends on the specimen geometry. β value is closely related to the volume fraction of inclusion.

(2) The J-resistance curve of the true crack length obtained from the linear roughness is more conservative than that of the conventional crack length and shows a good agreement with the prediction of RDDT.

Reference

Bilby, B. A., et al., 1993. "Prediction of the First Spinning Cylinder Test Using Ductile Damage Theory," *Fatigue And Fracture of Engineering Materials and Structures*, 16, pp. 1~20.

Devaux, J. C. et al., 1985, "Experimental and Numerical Validation of Local Ductile Fracture Criterion Based on Simulation of Cavity Growth," *Nonlinear Fracture Mechanics*: V. II, ASTM STP 995, J. D. edited by Landes et al. pp. 7~23.

Franklin, A. G., 1969, "Comparison Between a Quantitative Microscope and Chemical Methods for Assessment of Non-Metallic Inclusions," *Journal of Iron and Steel Institues*, pp. 181 ~186.

Han-Ki Yoon et al, , 1999, "Evaluation on Elastic Fracture Toughness of SA533B-1 Steel by Load Ratio Analysis and Multiple Specimen Method," *Journal of KSME*, Vol. 23, No. 9, pp. 1598~1605.

Hay, E. et al., 1981, "A D. C. Potential Drop Method to Monitor Crack Growth in Notches Subjected to Torsion," *Fatigue and Fracture of Engineering Materials and Structures 4, pp. 287 ~290.*

Li. at al, , 1994, "A Study of the Internal Parameters of Ductile Damage Theory," *Fatigue Fract. Mater. Struct.* 17 pp. 1075~1087.

Rousellier, G., 1987, "Ductile fracture models and their potential in-local approach of fracture" *Nuclear Engineering and Design*, 105: pp. 97 ~111.

Suresh, S. et al., 1987, "Combined Mode I-Mode III Fracture of Fatigue Precracked Alumina," *Journal of American Ceramic Society*, 70, pp. 726~733.

Underwood, E. E., et al., 1985, "Quantitative Fractography," *ASM Metals Handbook 12 Fractography* (9th Ed.) pp. 193~210.